Mutant p53 improves cancer cells' resistance to endoplasmic reticulum stress by sustaining activation of the UPR regulator ATF6

Daria Sicari[1,2] · Marco Fantuz[1,2,3] · Arianna Bellazzo[1,2] · Elena Valentino[1,2] · Mattia Apollonio[1,2] · Ilaria Pontisso[1,2] · Francesca Di Cristino[1,2] · Marco Dal Ferro[2] · Silvio Bicciato[4] · Giannino Del Sal[1,2,5] · Licio Collavin[1,2]

Accepted: 30 June 2019

Abstract

Missense mutations in the TP53 gene are frequent in human cancers, giving rise to mutant p53 proteins that can acquire oncogenic properties. Gain of function mutant p53 proteins can enhance tumour aggressiveness by promoting cell invasion, metastasis and chemoresistance. Accumulating evidences indicate that mutant p53 proteins can also modulate cell homeostatic processes, suggesting that missense p53 mutation may increase resistance of tumour cells to intrinsic and extrinsic cancer-related stress conditions, thus offering a selective advantage. Here we provide evidence that mutant p53 proteins can modulate the Unfolded Protein Response (UPR) to increase cell survival upon Endoplasmic Reticulum (ER) stress, a condition to which cancer cells are exposed during tumour formation and progression, as well as during therapy. Mechanistically, this action of mutant p53 is due to enhanced activation of the pro-survival UPR effector ATF6, coordinated with inhibition of the pro-apoptotic UPR effectors JNK and CHOP. In a triple-negative breast cancer cell model with missense TP53 mutation, we found that ATF6 activity is necessary for viability and invasion phenotypes. Together, these findings suggest that ATF6 inhibitors might be combined with mutant p53-targeting drugs to specifically sensitise cancer cells to endogenous or chemotherapy-induced ER stress.

Introduction

In eukaryotic cells, the endoplasmic reticulum (ER) performs crucial activities such as lipid biosynthesis, calcium storage, and protein folding and secretion. Homeostasis of these processes is strictly regulated, and their alterations generate a condition referred to as endoplasmic reticulum stress (ERS) [1]. To cope with ER stress, cells activate a specific transcriptional programme known as Unfolded Protein Response (UPR). The UPR is initiated by three independent ER-resident transmembrane proteins: inositol-requiring enzyme-1 (IRE1), PKR-like ER kinase (PERK) and activating transcription factor-6 (ATF6). These sensors regulate mutually reinforcing signalling pathways and transcriptional circuits aimed, at first, to resolve the stress; when the burden cannot be resolved, apoptotic cell death occurs [2].

IRE1α, the more evolutionarily conserved UPR receptor, has both endoribonuclease and protein-kinase activities: the former mediates cytoplasmic splicing of the Xbp1 mRNA to generate the transcriptional regulator XBP1s [3], the latter triggers activation of the pro-apoptotic kinase JNK by recruitment of the TRAF2/ASK1 complex [4].

The second UPR receptor, PERK, when activated phosphorylates the α-subunit of eukaryotic translation initiation factor-2 (eIF2α); this attenuates mRNA translation, thus reducing protein load [5]. Although cap-dependent translation is inhibited, synthesis of selected transcripts is increased; in particular, the transcription factor

✉ Giannino Del Sal
giannino.delsal@Lncib.it

✉ Licio Collavin
collavin@Lncib.it

1 National Laboratory CIB (LNCIB), AREA Science Park, 34149 Trieste, Italy

2 Department of Life Sciences, University of Trieste, 34127 Trieste, Italy

3 International School for Advanced Studies (SISSA), Trieste, Italy

4 Department of Life Sciences, University of Modena and Reggio Emilia, 41100 Modena, Italy

5 IFOM, the FIRC Institute of Molecular Oncology, Trieste, Italy

ATF4 is strongly induced upon eIF2α phosphorylation. ATF4 in turn upregulates ER chaperones and pro-apoptotic genes such as CHOP/GADD153 [6].

The third UPR receptor is the transcription factor ATF6, which is synthesised as an ER-localised transmembrane protein with a luminal "sensing" domain and a cytosolic transcription transactivation domain [7]. Under ER stress conditions, ATF6 translocates to the Golgi apparatus, where it is cleaved by S1P and S2P proteases [8]. The cleavage product (p50 ATF6f) is transported into the nucleus where it drives transcription of ER chaperones, ERAD components, the pro-apoptotic factor CHOP, and several other homeostatic effectors [9].

Cancer cells within tumour masses experience chronic ER stress due to adverse conditions such as nutrient deprivation, oxygen limitation, and high metabolic demand, all of which reduce the protein-folding capability of the ER [10]. Moreover, transformed cells accumulate hundreds of mutations, potentially generating aberrant proteins that cannot properly fold [11]. Not surprisingly, ERS responses have been reported in all major cancer types [12], often correlating with advanced-stage disease and chemoresistance [13]. This suggests that cancer cells eventually adapt to ER stress, avoiding the pro-apoptotic outcomes of UPR. In addition, there are evidences that ERS-related pathways may actually promote cancer progression by inducing EMT, stimulating angiogenesis and supporting tumour cell dormancy [14]. Therefore, understanding the genetic determinants that dictate adaptation of cancer cells to ER stress is critical for developing novel clinical strategies.

One of the most frequently mutated genes in human cancer is TP53, and strong evidences implicate missense p53 mutants as promoters of aggressive and metastatic phenotypes. Indeed, p53 mutant proteins (mutp53) can acquire novel oncogenic activities, defined as Gain of Function (GOF), that actively promote cancer development and progression [15, 16].

Recent studies revealed GOF activities for mutant p53 in processes involved in the maintenance of cell homeostasis [17], including inflammatory signalling [18, 19], response to mechanical stress [20], proteasome activity [21] and folding of N-glycosylated proteins [22]. Based on these premises, we asked whether mutant p53 might intersect the UPR to promote cancer cells' resistance to ER stress.

Results

Mutant p53 protects cancer cells from ER stress-induced apoptosis

To explore the role of mutp53 in the response of cancer cells to ER stress, we performed viability assays in the human triple-negative breast cancer (TNBC) cell line MDA-MB-231, bearing mutant p53(R280K). To induce ER stress, cells were treated with Thapsigargin (Tg) or Tunicamycin (Tm) for 48 hours. Under these conditions, depletion of endogenous mutant p53 reduced viability and increased apoptosis (Fig. 1a, b), suggesting that mutp53 protects these cells from this specific stress. We obtained similar results in two additional mutant p53 cancer cell lines, SUM-149PT (p53M237I) and PANC-1 (p53R273H), and we confirmed this observation in Ras-transformed mouse embryo fibroblasts (MEFs) derived from p53 knock-out or p53(R172H) knock-in mice (Fig. S1a–c). Therefore, this phenotype is not restricted to breast cancer cells.

Next, we transduced two mutant p53 variants (R280K and R175H) in HBL-100, a transformed mammary cell line with wild-type (wt) p53; in this model, ectopic expression of mutp53 was sufficient to enhance resistance to ER stress (Fig. 1c). Together, these observations indicate that mutant p53 can be a determinant of cancer cell survival under conditions of ER stress, potentially defining a novel mutp53 gain of function.

Cell responses to ER stress are largely mediated by activation of the UPR; we therefore evaluated whether mutant p53 might directly or indirectly affect expression of UPR genes. Taking advantage of available transcriptomic data from a previous study [21], we monitored changes in UPR-related genes upon depletion of endogenous mutp53 in five different TNBC cell lines (see methods for details). In all of the cell lines, UPR-related genes were significantly affected by mutp53 depletion (Fig. 1d, Table S1), some of them being repressed while others being induced (Table S2). Notably, the UPR receptors IRE1α and PERK were upregulated after mutp53 knockdown in MDA-MB-231 cells; this observation was validated experimentally both at the mRNA and protein levels (Fig. 1e and S1d).

Mutant p53 dampens IRE1α- and PERK-related signalling

IRE1α and PERK and have similar activation mechanisms, and can induce either adaptive or pro-apoptotic responses [1]. To monitor their function, we analysed a panel of downstream effectors in MDA-MB-231 cells depleted for mutant p53. Interestingly, mutp53 knockdown enhanced the transcription of CHOP, a target of PERK, and the production of spliced XBP1 (XBP1s), a target of IRE1α (Fig. 2a and S2a), confirming activation of the two receptors. In line with higher PERK activity, mutp53 depletion increased the phosphorylation of eIF2-alpha (Fig. S2b). Mutant p53 knockdown also enhanced the kinase activity of IRE1α, increasing the phosphorylation of its downstream target JNK (Fig. 2b and S2c); coherently, reintroduction of mutant p53(R280K) in MDA-MB-231 cells depleted of endogenous mutp53 reduced the amplitude of ERS-induced JNK activation (Fig. 2c).

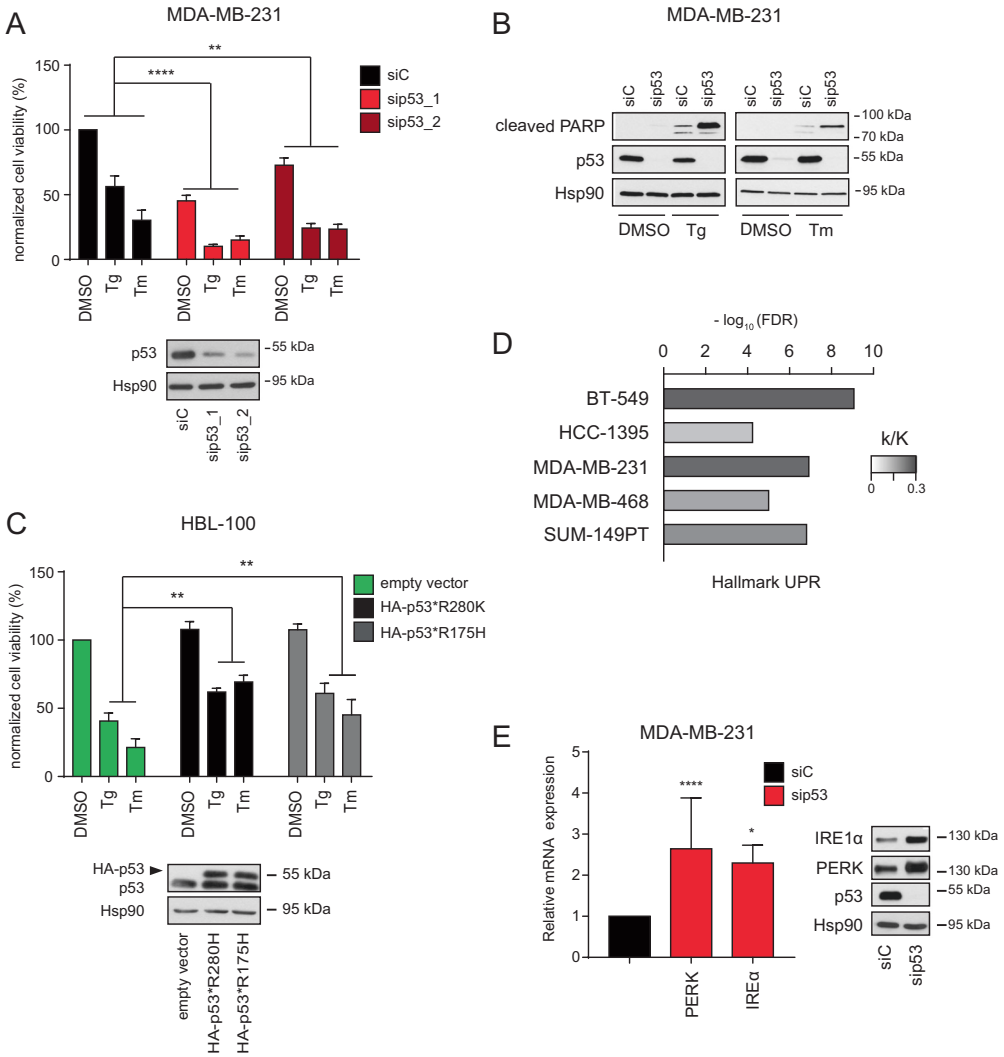

Fig. 1 Mutant p53 promotes cancer cells' survival under ER stress (ERS). **a**, **b** Mutant p53 knockdown reduces cancer cell viability and increases ERS-induced apoptosis. **a** MDA-MB-231 cells were transfected with control (siC) or two different p53 siRNAs (sip53) as indicated. 48 hours post-transfection, cells were seeded in 96-well plates and treated with DMSO (vehicle), Thapsigargin (Tg, 1 µM) or Tunicamycin (Tm, 5 µg/ml) for additional 48 hours. Cell viability was measured by ATP-lite assays; graphs summarise cell viability normalised to siC-transfected untreated cells (mean ± SD; $n = 3$; $^{***}P < 0.001$, $^{**}P < 0.01$). **b** MDA-MB-231 cells were treated as in **a** and analysed by western blot. Cleaved PARP was blotted as a marker of apoptosis. p53 was blotted to monitor knockdown efficiency, with Hsp90 as loading control. **c** Mutant p53 overexpression protects cells from ER stress. HBL-100 cells were stably transduced with retroviral vectors encoding mutant p53 (R280K) or p53 (R175H) as indicated. Cells were treated and analysed as in **a** (mean ± SD; $n = 3$; $^{**}p < 0.01$). **d** Depletion of mutant p53 affects expression of UPR genes. Genes differentially regulated upon mutp53 depletion in five TNBC cell lines were subjected to an hypergeometric test for computing overlaps with the geneset "Hallmark Unfolded Protein Response" from MsigDB. Functional enrichment is plotted as –log (FDR q-value). Colour of the bars reflects the cluster coverage (k/K). **e** Depletion of mutant p53 increases IRE1α and PERK levels. MDA-MB-231 cells were transfected with control (siC) or p53 (sip53) siRNAs for 48 hours before analysis. RT-qPCR data are normalised to H3 mRNA, and compared to the expression levels of untreated cells transfected with siC. Immunoblots are normalised using Hsp90 as a loading control

In line with the above observations, overexpression of mutant p53(R280K) in p53-null H1299 cells gave an opposite phenotype, with less efficient induction of CHOP and XBP1s upon ER stress (Fig. 2d). Together, these results suggest that mutp53 inhibits the IRE1α and PERK branches of the UPR, dampening activation of two key pro-apoptotic effectors such as CHOP and JNK [4, 6].

We therefore assessed the role of CHOP and JNK in ERS-induced apoptosis in mutp53-depleted cancer cells. Interestingly, siRNA knockdown of either JNK or CHOP was sufficient to reduce Tg- or Tm- induced cell death after mutp53 knockdown, partially rescuing the impact of mutant p53 loss (Fig. 2e, f). This indicates that both JNK and CHOP contribute to the enhanced sensitivity to ER stress observed in mutp53 knockdown cancer cells.

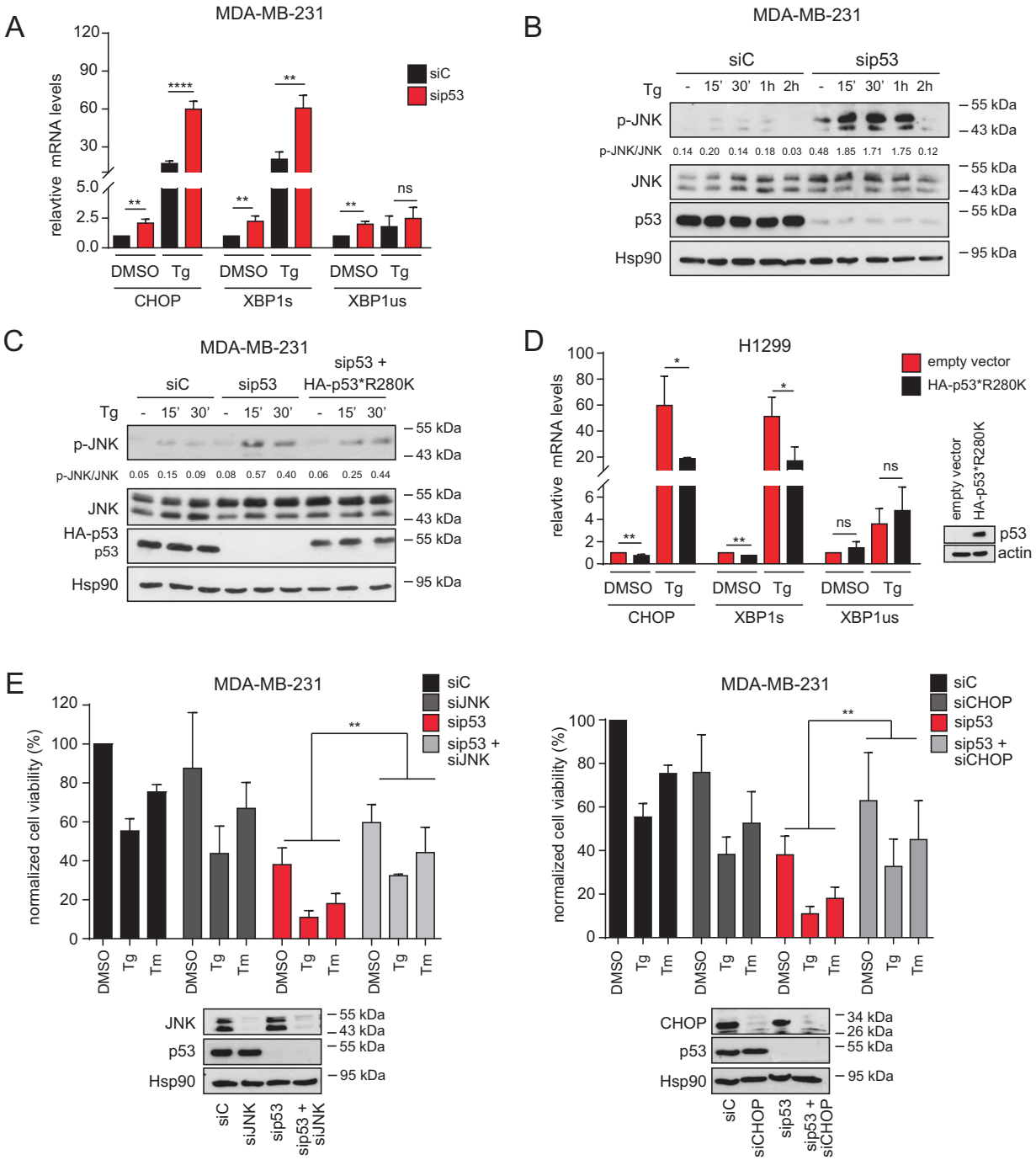

Fig. 2 Mutant p53 dampens IRE1- and PERK-related signalling. **a** Mutp53 depletion increases CHOP and XBP1s mRNA levels. MDA-MB-231 cells were transfected with control (siC) or p53 (sip53) siRNAs for 48 hours, and treated with Tg (1 μM) for additional 8 hours. RT-qPCR data are normalised to H3 mRNA (mean ± SD; $n \geq 3$, $^{**}p < 0.01$, $^{***}p < 0.001$; $^{****}p < 0.0001$; ns = not significant). **b** Mutp53 depletion increases ERS-induced JNK phosphorylation. MDA-MB-231 were transfected with control (siC) or p53 (sip53) siRNAs for 48 hours, and treated with Tg for the indicated times. Phosphorylated and total JNK levels were measured by immunoblotting; to calculate their ratio, bands were quantified and normalised to Hsp90 by densitometry of autoradiography film. Endogenous p53 was blotted to verify knockdown, Hsp90 as a loading control. **c** Ectopic reintroduction of mutant p53 dampens ERS-induced JNK activation in mutp53 knockdown cells. MDA-MB-231 were transfected with control (siC) or p53 (sip53) siRNAs. After 24 hours, cells were transfected with pLPC-empty vector or pLPC-HA-p53*R280K, encoding a siRNA-resistant (*) p53 mutant. Lysates were prepared after treatment with Tg for the indicated times. Phosphorylated and total JNK levels were measured by immunoblotting and quantified as in **b**. **d** Mutant p53 overexpression decreases CHOP and XBP1s mRNA levels. H1299 were stably transduced with retroviruses encoding mutant p53(R280K) or p53(R175H). Cells were treated and analysed as in **a** (mean ± SD; $n = 3$; $^{*}p < 0.05$; $^{**}p < 0.01$). **e** Both JNK and CHOP mediate ERS-induced apoptosis in mutp53-depleted cancer cells. MDA-MB-231 were transfected with the indicated siRNA combinations for 48 hours, and were treated and analysed for viability as in Fig. 1a (mean ± SD; $n = 3$; $^{**}p < 0.01$)

Mutant p53 sustains ATF6 activation

Having established that mutant p53 can dampen the activity of IRE1α and PERK receptors, we asked if mutp53 could also impact on ATF6 functions. To monitor ATF6 activation we used a luciferase reporter plasmid with five repetitions of the ATF6 responsive element [23]. Notably, reporter activity was sensibly reduced by mutp53 knockdown in MDA-MB-231 cells, both in basal conditions and upon ER stress (Figs. 3a and S3a). Similar results were obtained by depleting mutp53 in MDA-MB-468 cells (Fig. S3b). Conversely, overexpression of two different missense p53 mutants in p53 wild-type (HBL-100) or p53-null (H1299) cells resulted in increased ATF6 transcriptional activity (Figs. 3b and S3c). Together, these data indicate that mutp53 enhances ATF6 activation.

Since activation of ATF6 requires its proteolytic processing to release the transcriptionally active fragment p50-ATF6, or ATF6f [7], we analysed expression of ATF6 proteins after mutant p53 depletion in MDA-MB-231. Notably, mutp53 knockdown induced a clear reduction of ATF6f levels (Fig. 3c), without significant changes in ATF6 mRNA or full-length protein (Fig. S3d). To better address this point, we analysed the kinetics of ERS-induced ATF6 cleavage in MDA-MB-231 cells; results indicate that ATF6 processing occurs at similar times after ER stress, but the levels of p50 ATF6f are significantly lower after mutp53 depletion (Figs. 3d and S3e–g).

To test if mutant p53 may dominantly promote ATF6 activation, we analysed ATF6f levels in HBL-100 (wt p53) stably overexpressing two different p53 mutants (R280K and R175H); in these cells, mutp53 clearly increased ATF6f production (Fig. 3e). We thus conclude that oncogenic p53 mutants can enhance ATF6 function, increasing the levels of the active ATF6f fragment.

Based on the above, we searched for evidence of ATF6 activation in cancers with mutant p53. To this aim, we analysed public breast cancer gene expression datasets with reliable information on the p53 status: the METABRIC study [25], and the BRCA cohort of TCGA [26]. We divided samples based on the status of p53, and measured average expression of two publicly available lists of ATF6 target genes (see Supplementary methods for details). As shown in Fig. 3f, both gene signatures are more expressed in tumours with missense TP53 mutations, in line with the notion that mutp53 can sustain ATF6 activation.

ATF6 activity is required for cancer cell survival and invasion

ATF6 induces expression of various chaperones and protein quality control genes [9, 27]; we therefore hypothesised that mutant p53 may sustain oncogenic adaptation to ER stress, at least in part, by promoting ATF6-dependent homeostatic responses. To test this hypothesis, we studied the effects of ATF6 depletion in MDA-MB-231 cells. We first analysed cell survival; we found that ATF6 knockdown reduced basal viability of these cells and, importantly, increased their sensitivity to ER stress (Fig. 4a). Next, we analysed cell invasivity by matrigel transwell assays; notably, ATF6 knockdown caused a substantial reduction in the number of invaded cells (Fig. 4b). Therefore, ATF6 is required for full manifestation of mutp53-dependent oncogenic phenotypes of MDA-MB-231 cells.

Importantly, this observation was confirmed with mutp53 overexpression in a p53-null cell line; in fact, transfection of p53(R280K) increased matrigel invasion of H1299 cells, and this effect was abolished by ATF6 knockdown (Fig. 4c). Finally, we tested the effects of ATF6 overexpression in MCF-7, a breast cancer cell line with wt p53 and limited invasive potential; in these cells, transfection of a GFP-ATF6 fusion protein was sufficient to increase matrigel invasion (Fig. 4d). Together, these data suggest that resistance to ER stress in cancer cells with mutant p53 depends not only on reduced IRE1 and PERK function, but also on increased ATF6 activity; remarkably, they also suggest that ATF6 could directly contribute to mutp53-related aggressiveness.

Small molecule inhibitors of mutant p53 or ATF6 reduce cancer cells survival and aggressiveness

ER stress can theoretically be exploited to selectively target tumour cells [11]. We therefore tested the possibility to sensitise cancer cells to ER stress by acting on mutant p53 or ATF6 using currently available drugs.

To target mutant p53, we used the FDA-approved histone-deacetylase inhibitor Suberoyl Anilide Hydroxamic Acid (SAHA), a drug that reduces mutp53 protein levels and shows preferential cytotoxicity in mutant p53 cancer cells [28]. To target ATF6, we used Nelfinavir (NFV), an anti-viral drug that inhibits S1P and S2P proteases responsible for ATF6 cleavage [29, 30].

First, to choose optimal concentrations of each drug, we performed dose-response experiments in MDA-MB-231 cells (Fig. S4a). Next, to evaluate the impact of pharmacological mutp53 inhibition, we tested cell viability upon treatment with SAHA, alone or in combination with ER stressors; as expected, SAHA increased sensitivity of MDA-MB-231 to ER stress, recapitulating the effects of mutp53 depletion (Fig. 5a). In line with knockdown experiments, treatment with SAHA also reduced ATF6f levels and transactivation of the ATF6-LUC reporter (Fig. 5b, c). As a control, we tested SAHA in cells that do not express mutant p53, specifically H1299 (p53-null) and HBL-100 (wt p53); we detected some

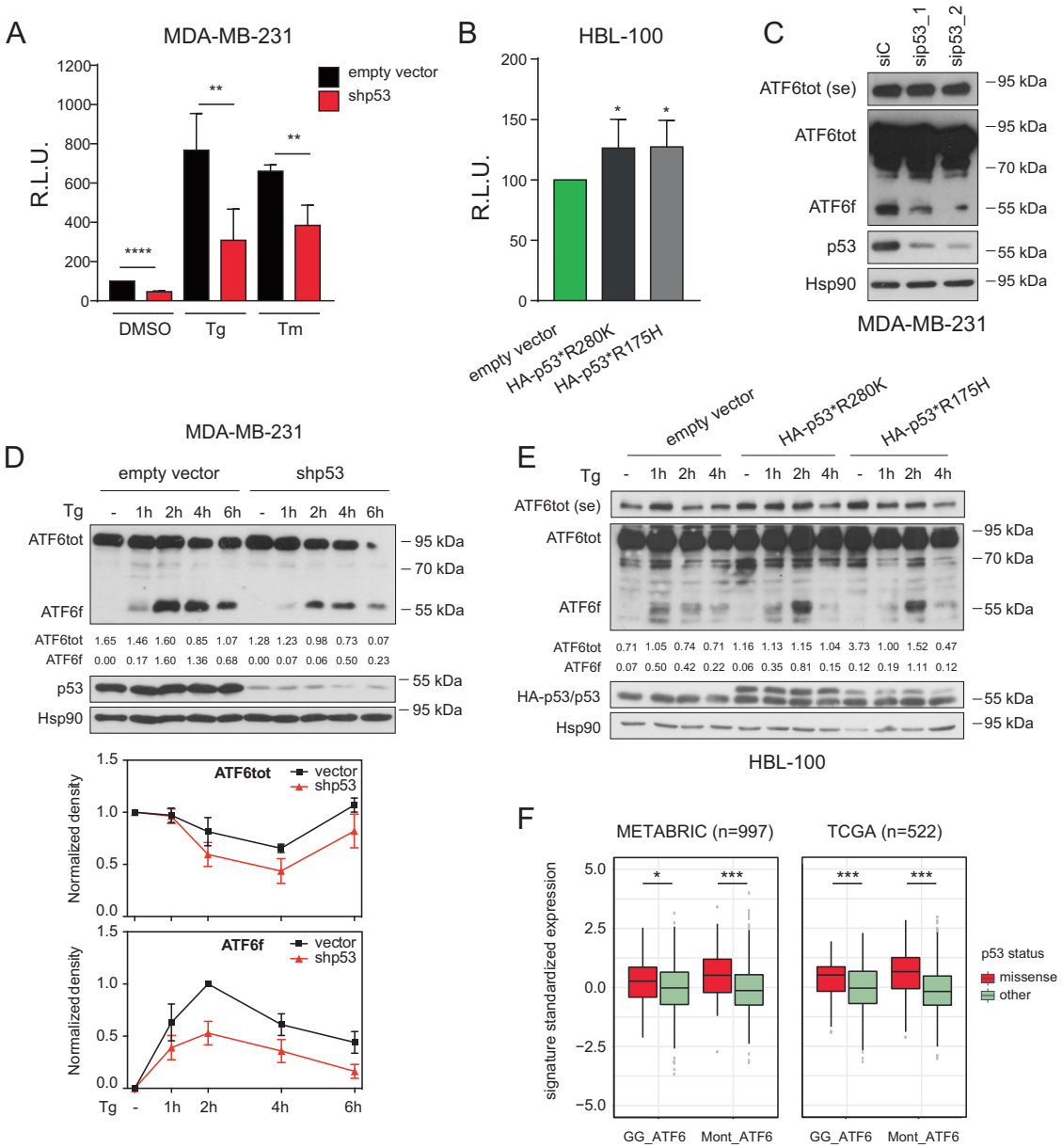

Fig. 3 Mutant p53 sustains ATF6 activation. **a** Depletion of mutant p53 reduces ATF6 transcriptional activity. MDA-MB-231 cells, stably depleted for p53 (shp53) or stably expressing control empty vector, were transfected with the p5×ATF6-GL3 reporter to detect ATF6 transcriptional activity. After 48 hours, cells were treated with DMSO (vehicle), Tg (1 µM) or Tm (5 µg/ml) for 8 hours before processing for Dual Luciferase assays (mean ± SD; $n = 3$; $^{**}p < 0.01$; $^{****}p < 0.0001$). **b** Mutant p53 overexpression increases ATF6 transcriptional activity. HBL-100 cells were stably transduced with retroviruses encoding mutant p53(R280K) or p53(R175H). Cells were then transiently transfected with p5×ATF6-GL3 to detect ATF6 transcriptional activity as in **a** (mean ± SD; $n = 4$; $^{*}p < 0.05$,). **c** Depletion of mutant p53 reduces basal ATF6 processing. MDA-MB-231 cells were transfected with control (siC) or two different p53 (sip53) siRNAs as indicated. Full-length p90 ATF6 (ATF6tot) and cleaved p50 ATF6 (ATF6f) were detected by immunoblotting. p53 was blotted to monitor knockdown efficiency, Hsp90 as a loading control (se = short exposure). **d** Depletion of mutant p53 reduces ERS-induced ATF6 cleavage. MDA-MB-231 cells expressing a control vector or stably depleted for p53 (shp53) were treated with Tg for the indicated times. ATF6tot and ATF6f were detected by immunoblotting; bands were quantified and normalised to Hsp90 by densitometry of autoradiography film. Top panel shows a representative western blot. Bottom graphs summarise the relative levels of ATF6tot and ATF6f bands at the indicated times, with ATF6tot normalised to untreated control cells and ATF6f normalised to the 2 hours time point in control cells (mean ± SEM; $n = 4$). **e** Mutant p53 overexpression increases ATF6 production. HBL-100 cells were transduced with retroviruses encoding mutant p53(R280K) or p53(R175H) as indicated. After 48 hours, cells were treated with Tg for the indicated times before immunoblotting to detect full-length and cleaved ATF6 as in **d**. **f** ATF6 target genes are more expressed in breast tumours with mutant p53. Average expression values of ATF6 signatures in breast cancer samples classified according to p53 status ($^{*}p < 0.05$, $^{***}p < 0.001$ in a two-tailed unpaired *t*-test). METABRIC = Molecular Taxonomy of Breast Cancer International Consortium. TCGA = The Cancer Genome Atlas project. GG_ATF6 = Selected GeneGlobe predicted target genes for ATF6 (www.genecards.org). Mont_ATF6 = Manually curated list of ATF6 target genes [24]

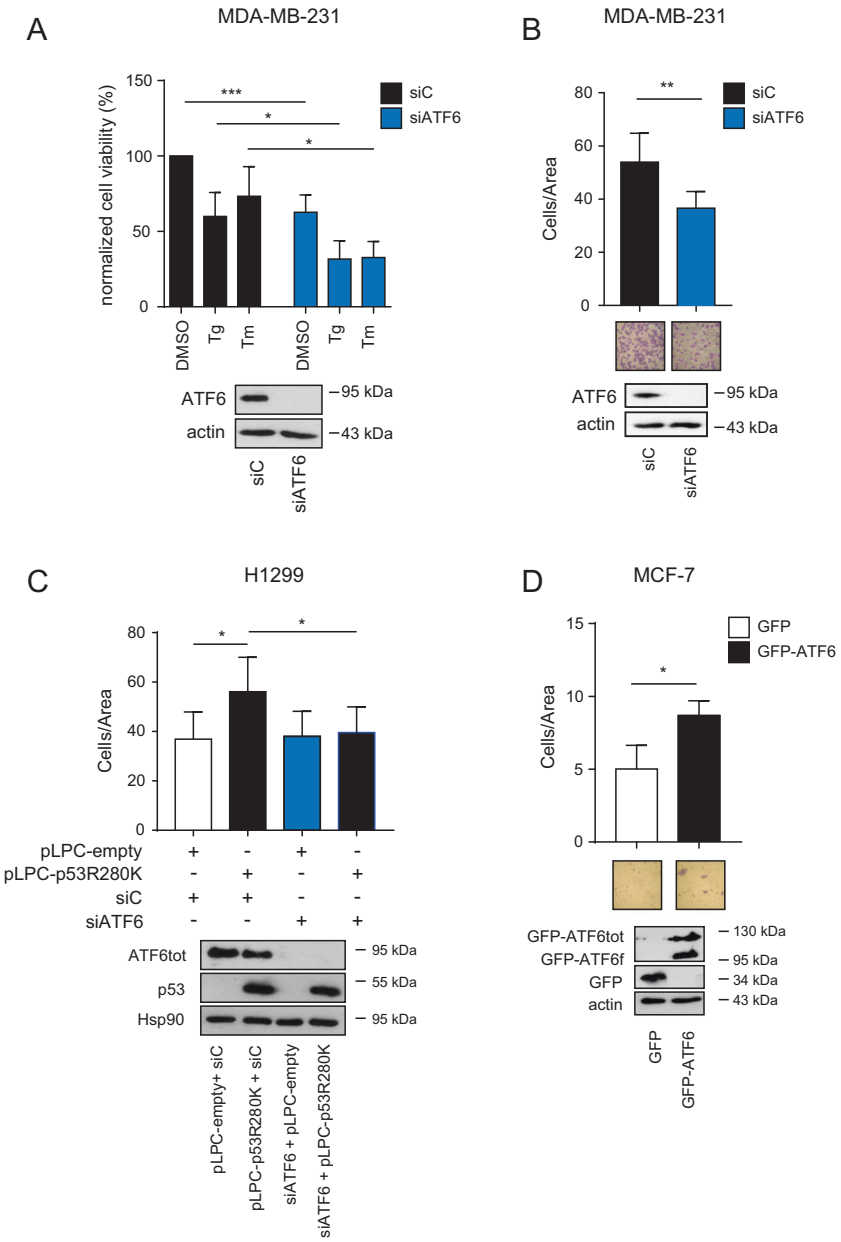

Fig. 4 ATF6 activity supports cancer cells' viability and invasion. **a** ATF6 depletion reduces cell viability upon ER stress. MDA-MB-231 cells were transfected with control (siC) or ATF6 (siATF6) siRNAs for 48 hours. Cells were treated and analysed for viability as in Fig. 1a (mean ± SD; $n = 4$; $*p < 0.05$; $***p < 0.001$). **b** ATF6 depletion reduces matrigel invasion. MDA-MB-231 cells were transfected with control or ATF6 siRNA as in **a**. Graphs summarise migrated cells per area (mean ± SD; $n = 4$; $**p < 0.01$). Depletion of endogenous ATF6 was confirmed by western blot. Representative images of migrated cells are also shown. **c** ATF6 contributes to mutp53-induced cell invasion. H1299 (p53-null) cells were transiently transfected with a vector encoding mutant p53(R280K) and/or ATF6 siRNA as indicated. Matrigel invasion assays were performed 24 hours later. Graphs summarise migrated cells per area (mean ± SD; $n = 3$; $*p < 0.05$). Expression of endogenous ATF6 and exogenous mutp53 proteins was monitored by immunoblotting (bottom panel). **d** ATF6 overexpression increases cancer cell invasiveness. MCF-7 cells (wt p53) were transiently transfected with a pEGFP-ATF6 expression construct. After 24 hours, cells were seeded for matrigel invasion assays. Graphs summarise migrated cells per area (mean ± SD; $n = 3$; $*p < 0.05$). Expression of GFP-ATF6 fusion proteins was monitored by immunoblotting (bottom panel). Representative images of migrated cells are also shown

inhibition of the ATF6-LUC construct in these cells, albeit below the threshold of statistical significance (Fig. S4b). Although we cannot exclude that SAHA has some mutp53-independent effects on ATF6 activity, it is legitimate to assume that its action in cells expressing mutant p53 is largely mediated by mutp53 downregulation.

Similarly, to evaluate the impact of pharmacological ATF6 inhibition, we tested viability and invasiveness of

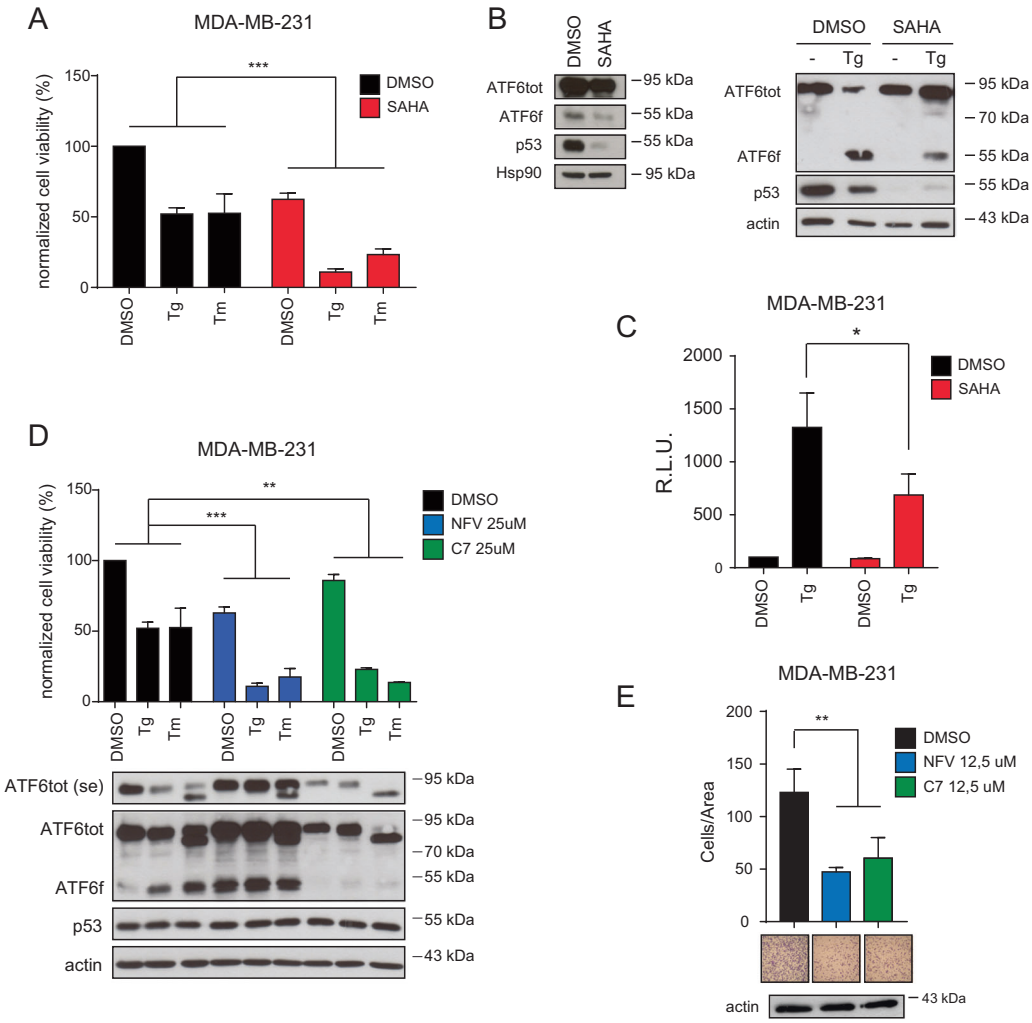

Fig. 5 Effects of pharmacological inhibitors of mutant p53 and ATF6. **a** The histone-deacetylase inhibitor SAHA reduces cell survival upon ER stress. MDA-MB-231 cells were treated with DMSO (vehicle), Tg (1 μM) or Tm (5 μg/ml), with or without SAHA (1 μM) as indicated. After 48 hours, cell viability was measured as in Fig. 1a (mean ± SD; $n = 3$; $^{***}p < 0.001$). **b** SAHA reduces ATF6 cleavage. Left: steady-state levels of endogenous full-length and cleaved ATF6 were detected by immunoblotting after 48 hours of SAHA treatment in the absence of ERS-inducing drugs. Right: endogenous full-length and cleaved ATF6 were detected by immunoblotting after 72 hours treatment with SAHA, and additional 2 hours with Tg. Mutant p53 was blotted to monitor SAHA efficacy, with Hsp90 or actin as loading controls. **c** SAHA inhibits ATF6 transcriptional activity. MDA-MB-231 cells were transfected with the p5xATF6-GL3 and after 48 hours treated with SAHA for additional 24 hours. ATF6f transcriptional activity was measured by Dual Luciferase assay after 8 hours of Tg treatment (mean ± SD; $n = 3$; $^{*}p < 0.05$). **d** The ATF6 inhibitors Nelfinavir (NFV) and Ceapin-A7 (C7) reduce cell survival upon ER stress. MDA-MB-231 cells were treated with DMSO (vehicle), Tg (1 μM) or Tm (5 μg/ml), with or without NFV (25 μM) or C7 (25 μM) as indicated. After 48 hours, cell viability was measured as in Fig. 1a (mean ± SD; $n = 3$; $^{***}p < 0.001$ $^{**}p < 0.01$). Bottom panel shows expression of endogenous ATF6 and p53 proteins under the same treatment conditions, with actin as loading control (se = short exposure). **e** ATF6 pharmacological inhibition reduces matrigel invasion. MDA-MB-231 cells were pre-treated for 24 hours with DMSO (vehicle), NFV (12,5 μM), or C7 (12,5 μM) as indicated. Graphs summarise migrated cells per area (mean ± SD; $n = 3$; $^{**}p < 0.01$). Actin was blotted as a control of the number of cells seeded in transwell inserts. Representative images of migrated cells are also shown

MDA-MB-231 cells treated with NFV, alone or in combination with ERS-inducing drugs. We also used the highly specific ATF6 inhibitor Ceapin-A7 (C7) as a positive control [31]. Strikingly, both drugs phenocopied ATF6 knockdown, reducing cell survival and invasion (Fig. 5d, e). As expected, NFV and C7 inhibited ERS-induced cleavage of a GFP-ATF6 fusion protein, and prevented activation of the ATF6-LUC reporter (Fig. S4c, d).

Combined targeting of mutant p53 and ATF6 sensitises cancer cells to ER stress

Since SAHA and NFV act on different molecular targets, we also tested their combined use. Viability assays revealed that treatment with the two compounds was more efficient in reducing MDA-MB-231 viability than treatment with single drugs - in particular upon ER stress (Fig. 6a).

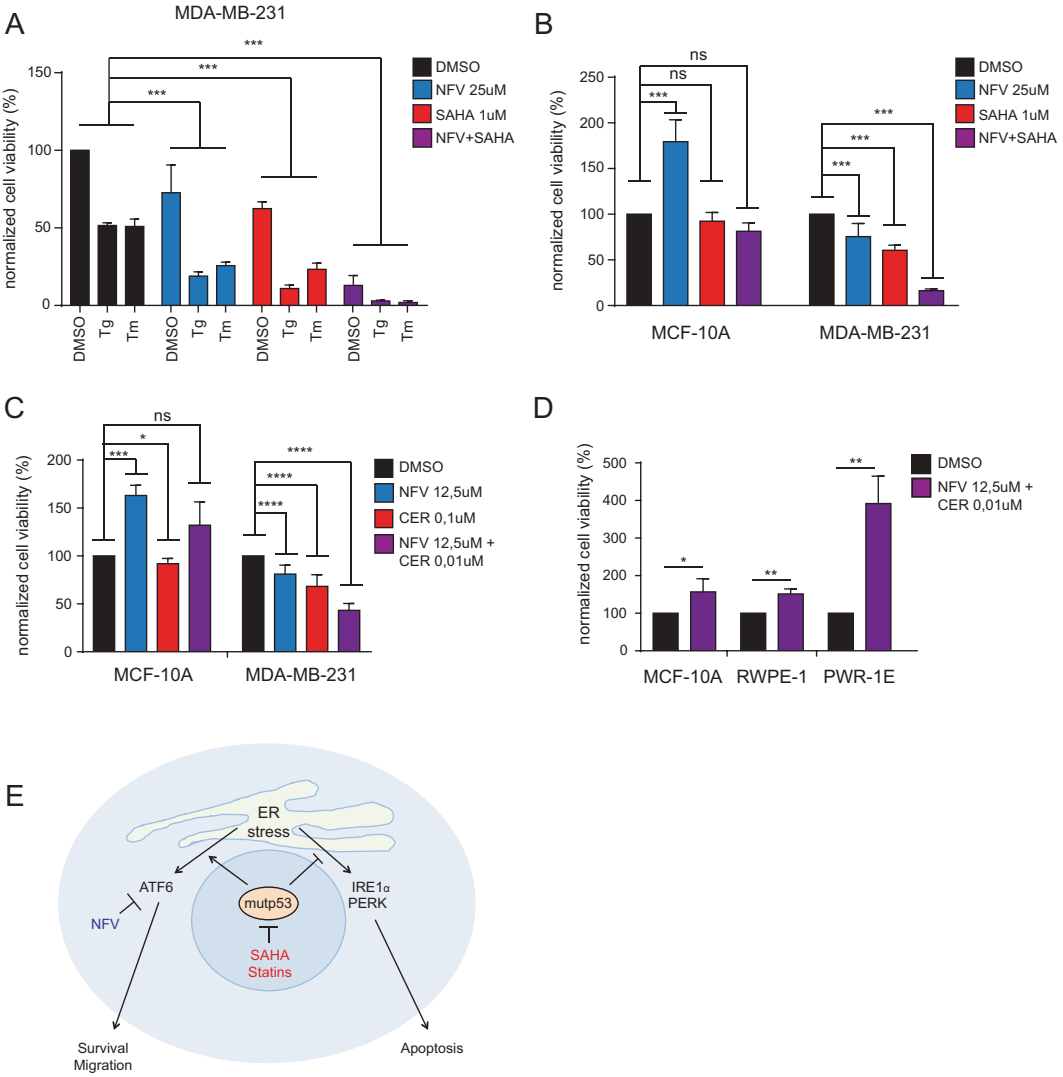

Fig. 6 Combined targeting of mutant p53 and ATF6 efficiently and specifically sensitises cancer cells to ER stress. **a** SAHA and NFV cooperatively reduce cancer cells survival upon ER stress. MDA-MB-231 cells were treated for 48 hours with DMSO (vehicle), SAHA (1 μM) and/or NFV (25 μM), and Tg (1 μM) or Tm (5 μg/ml) as indicated. Cell viability was measured by ATP-lite assays as in Fig. 1a (mean ± SD; $n = 3$; $^{***}p < 0.001$). **b** SAHA and NFV do not affect viability of non-transformed cells upon ER stress. Breast epithelial cells MCF10-A were treated and analysed exactly as in **a** (mean ± SD; $n = 3$; $^{***}p < 0.001$, $^{**}p < 0.01$). **c** MCF-10A and MDA-MB-231 cells were treated for 48 hours with DMSO (vehicle), CER (0,01 μM), or NFV (12,5 μM) as indicated. Cell viability was measured as in **a** (mean ± SD; $n = 3$; $^{***}p < 0.001$). **d** MCF-10A, RWPE-1 and PWR-1E cells were treated for 48 hours with DMSO (vehicle), CER (0,01 μM) or NFV (12,5 μM) as indicated. Cell viability was measured as in **a** (mean ± SD; $n = 3$; $^{***}p < 0.001$). **e** A simplified model of the influence of mutant p53 on the three branches of the UPR, and its potential impact on cellular responses to ER stress

Remarkably, calculation of the combination index (CI) [32] revealed that the two drugs have a synergic effect (Fig. S5a). Immunoblotting analysis confirmed the activity of NFV and C7 on ATF6 also in the presence of SAHA (Fig. S5b). To test if this effect is specific for cancer cells, we also treated the non-transformed mammary cell line MCF-10A; importantly, we observed no significant loss of MCF-10A viability under conditions that have a strong impact on MDA-MB-231 (Fig. 6b).

To reinforce these observations, we replaced SAHA with Cerivastatin (CER), a drug that inhibits mutp53 stability and functions indirectly by acting on the mevalonate pathway [20]. We tested CER alone or in combination with NFV, using low concentrations to minimise toxicity and highlight potential cooperative effects. Under these conditions, CER recapitulated the results obtained with SAHA, further reducing cell viability in MDA-MB-231 (Fig. 6c) without relevant effects in non-transformed breast or prostate cell lines (Fig. 6d).

Together, these data suggest that combined inhibition of mutp53 and ATF6 may specifically sensitise mutant p53 cancers to therapeutic treatments that increase ER stress, with marginal effects on normal tissue.

Discussion

Accumulating evidences indicate that mutant p53 proteins can act on molecular processes that control cancer cells' homeostasis, including the resistance to protein-related toxicity [17, 21, 22]. Here, we found that mutant p53 can modulate the cellular response to ER stress by affecting various components of the UPR. Specifically, mutp53 inhibits activation of the pro-apoptotic UPR effectors JNK and CHOP, and their upstream regulators IRE1α and PERK. At the same time, mutp53 stimulates activation of the pro-survival UPR effector ATF6.

The mechanism by which mutp53 dampens ERS-induced activation of JNK and CHOP remains to be defined. In some cell lines, mutp53 depletion increases IRE1α and PERK levels, suggesting that mutant p53 can inhibit expression of these receptors, which could in part contribute to their reduced activity. It is also possible that mutp53 indirectly dampens activation of pro-apoptotic UPR effectors by enhancing the homeostatic activity of ATF6 – thereby reducing the intensity of ER stress.

In addition to controlling ER homeostasis, activation of ATF6 can modulate apoptosis and autophagy [33–35], and various evidences implicate ATF6 in cancer. First, ATF6f is the main transcriptional regulator of the chaperone GRP78/BiP, which was found overexpressed in breast tumours correlating with STAT3 activation and cancer cell proliferation and migration [36]. Also, ATF6 was shown to support adaptation and chemoresistance of dormant squamous carcinoma cells via activation of mTOR signalling [37]. Finally, a recent study linked ATF6 activity to pluripotency, proliferation and survival of breast cancer stem cells [38].

Our experiments indicate that ATF6 is instrumental for at least two mutant p53 oncogenic phenotypes, namely resistance to ERS-inducing drugs and cell invasion. They also suggest that mutp53-bearing cancer cells rely on ATF6 to help resolve ER stress, and ATF6 activity might contribute to their aggressiveness.

The molecular mechanism by which mutant p53 promotes ATF6 activation remains to be defined, and will be the subject of future studies. Time-course experiments indicate that mutp53 depletion reduces the amount of p50 ATF6 fragment that is produced, without changing the kinetics of ERS-induced ATF6 cleavage. One possibility is that mutp53 stimulates ATF6 translocation to the Golgi. Alternatively, mutp53 could stimulate ATF6 processing independently of its Golgi localisation. Also, it is possible that mutant p53 controls activity, localisation, or stability of the mature ATF6f fragment. All these hypotheses await experimental testing.

Mutation of p53 inevitably implies loss of wild-type (wt) p53 functions. Although the role of wt p53 in the response to ER stress is still unclear, with evidence for p53 involvement [39, 40] and evidence for p53-independency [41, 42], we cannot exclude that loss of wt p53 per se can affect the UPR. However, in the present study we have depleted endogenous mutp53 in cancer cells, revealing a clear addiction to its UPR-related functions. Moreover, coherent results were obtained by introducing mutant p53 in p53-null or p53 wt cells. Therefore, we can reasonably affirm that the phenotypes described are linked to expression of mutant p53 proteins.

Given the complex interconnection between the three branches of UPR, and the fact that several target genes are co-regulated by multiple UPR effectors, it is difficult to establish whether ATF6 is indeed the key mediator of mutp53 gain-of-function in this context. Nonetheless, our data suggest that ATF6 may be targeted to reduce compensatory responses and increase therapeutic efficacy in mutant p53-bearing cancers; in fact, treatment with the ATF6 inhibitor Nelfinavir (NFV) combined with mutp53 inhibitors SAHA or Cerivastatin significantly increased ERS-induced cell death of a reference TNBC cell line.

We used NFV because it is approved for clinical use, but it is not a selective ATF6 inhibitor; thus, we cannot exclude an ATF6-independent action. Nonetheless, the highly specific ATF6 inhibitor Ceapin-A7 [31] gave identical results, strongly suggesting that the effects of NFV in this context are largely mediated by its action on ATF6.

In conclusion, we uncovered a novel functional axis linking mutant p53 to the UPR, with potentially oncogenic effects. A key node of this axis appears to be the transcription factor ATF6, which is a druggable target due to its specific mechanism of activation. Our results suggest that inhibition of ATF6 might potentially improve treatment of tumours harbouring TP53 gene mutations, and provide conceptual support to stimulate further research on specific ATF6-targeting drugs.

Materials and methods

Cell lines and drug treatments

The following human cell lines were used: MDA-MB-231 (p53R280K), MDA-MB-468 (p53R273H), SUM-149PT (p53M237I), PANC-1 (p53R273H), HBL-100 (wt p53), MCF-7 (wt p53), MCF-10A (wt p53), H1299 (p53 null), PWR-1E (wt p53), RWPE-1 (wt p53) and Ras-immortalised mouse embryonic fibroblasts (MEF) derived from p53 knock-out and p53R172H knock-in mice. To induce ER stress, cells were treated with 1 μM Thapsigargin (Sigma, T9033) or 5 μg/ml Tunicamycin (Sigma, T7765) unless differently specified. To inhibit ATF6 activation, cells were treated with 25 μM or 12.5 μM Nelfinavir mesylate hydrate (Sigma, PZ0013), or with 25 μM or 12.5 μM Ceapin-A7 (a

gift from Dr. Peter Walter), unless differently specified. To inhibit mutp53, cells were treated with 1 μM SAHA (Cayman, 149647-78-9), or with 0.01 μM or 0.1 μM Cerivastatin (Sigma, SML0005).

Cell viability and FACS analysis

For viability assay, we used ATP-lite Luminescence Assay System (PerkinElmer, 6016943). Cells were seeded in 96-well plates for 24 hours before treatments. ATP-lite reactions were performed according to the manufacturer instructions, and measured using an Enspire plate-reader (Perkin Elmer). For FACS analysis, adherent and floating cells were harvested, permeabilized with 0.1% NP-40 in PBS containing RNase A (200 μg/ml) and then stained with 50 μg/ml Propidium Iodide (#P4865, Sigma). At least 2×10^4 cells were counted in each experiment, using a FACSCalibur flow cytometer (Becton-Dickinson). Cell cycle analysis was performed with FlowJo software (http://www.flowjo.com/).

Matrigel invasion assays

Cells ($0.5–1 \times 10^5$) were plated in 24-well PET inserts (8 μm pore size, Falcon), coated with BD Matrigel (BD Bioscience). Cells were seeded in low serum (0.1% FBS), and the lower chamber was filled with high serum medium (10% FBS). After 16 h, cells passed through the filter were fixed in 4% PFA, stained with 0.05% crystal violet, and counted. Invasion was scored by counting cells in 20 random non-overlapping microscope fields at ×40 magnification.

Luciferase assays

The p5xATF6-GL3 reporter vector was a gift from Ron Prywes (Addgene plasmid #11976) [23]. For Dual Luciferase assays (Promega), cells were transfected with p5xATF6-GL3 together with pCMV-Renilla to normalise for transfection efficiency. Luciferase activity was measured on a Promega luminometer. For luciferase assays in siRNA-transfected cells, cells were transfected with the indicated siRNAs for 24 hours, washed from the transfection media, transfected with plasmid DNA, and collected 24 hours later.

Gene expression analysis

Total RNA was extracted with QIAzol (Qiagen). For RT-qPCR, 5μg of total RNA was reverse-transcribed with QuantiTect Reverse Transcription kit (Qiagen). Real-time PCR was performed using SsoAdvancedTMSYBR® Green Master Mix (Biorad) on a CFX96™ Real-Time PCR System (Biorad). Primer sequences are listed in Supplemental Experimental Procedures.

Statistical analysis

All experiments have been replicated at least three times. In graphs data are expressed as mean ± SD of three independent experiments, except when otherwise indicated. Differences were analysed by Student's *t*-test using Prism 7 (GraphPad), except when otherwise indicated. *P*-values < 0.05 were considered significant.

Acknowledgements We thank Giada Pastore (LNCIB, Trieste) for assistance with tissue culture. We thank Ciara Gallagher and Peter Walter (UCSF, USA) for kindly providing Ceapin-A7. We thank all people from LNCIB (Trieste) for advice and discussion. This work was funded by AIRC (Italian Association for Cancer Research) Investigator Grant (IG 14173) to LC, and AIRC Special Program Molecular Clinical Oncology "5 per mille" (Grant no. 10016) to GDS. This work was also funded by Regione FVG (LR 17/2014; project acronym RIFT) to GDS. AB was supported by a "G. Lucatello e G. Mazzega" postdoctoral fellowship from FIRC (Fondazione Italiana Ricerca sul Cancro), and by a Fondazione Umberto Veronesi postdoctoral fellowship. MF was supported by a "L. Fontana and M. Lionello" fellowship from FIRC. EV was supported by a "G. Lucatello e G. Mazzega" postdoctoral fellowship from FIRC.

Compliance with ethical standards

Conflict of interest The authors declare that they have no conflict of interest.

References

1. Bertolotti A, Zhang Y, Hendershot LM, Harding HP, Ron D. Dynamic interaction of BiP and ER stress transducers in the unfolded-protein response. Nat Cell Biol. 2000;2:326–32.
2. Walter P, Ron D. The unfolded protein response: from stress pathway to homeostatic regulation. Science. 2011;334:1081–6.
3. Prischi F, Nowak PR, Carrara M, Ali MMU. Phosphoregulation of Ire1 RNase splicing activity. Nat Commun. 2014;5:3554.
4. Urano F, Wang X, Bertolotti A, Zhang Y, Chung P, Harding HP, et al. Coupling of stress in the ER to activation of JNK protein kinases by transmembrane protein kinase IRE1. Science. 2000;287:664–6.
5. Harding HP, Zhang Y, Ron D. Protein translation and folding are coupled by an endoplasmic-reticulum-resident kinase. Nature. 1999;397:271–4.
6. Oyadomari S, Mori M. Roles of CHOP/GADD153 in endoplasmic reticulum stress. Cell Death Differ. 2004;11:381–9.
7. Haze K, Yoshida H, Yanagi H, Yura T, Mori K. Mammalian transcription factor ATF6 is synthesized as a transmembrane protein and activated by proteolysis in response to endoplasmic reticulum stress. Mol Biol Cell. 1999;10:3787–99.
8. Yoshida H, Okada T, Haze K, Yanagi H, Yura T, Negishi M, et al. ATF6 activated by proteolysis binds in the presence of NF-Y (CBF) directly to the cis-acting element responsible for the mammalian unfolded protein response. Mol Cell Biol. 2000;20:6755–67.
9. Wu J, Rutkowski DT, Dubois M, Swathirajan J, Saunders T, Wang J, et al. ATF6alpha optimizes long-term endoplasmic

reticulum function to protect cells from chronic stress. Dev Cell. 2007;13:351–64.
10. Chevet E, Hetz C, Samali A. Endoplasmic reticulum stress–activated cell reprogramming in oncogenesis. Cancer Discov. 2016;5:586–97.
11. Clarke Hanna J, Chambers Joseph E, Liniker E, Marciniak Stefan J. Endoplasmic reticulum stress in malignancy. Cancer Cell. 2014;25:563–73.
12. Wang M, Kaufman RJ. The impact of the endoplasmic reticulum protein-folding environment on cancer development. Nat Rev Cancer. 2014;14:581–97.
13. Urra H, Dufey E, Avril T, Chevet E, Hetz C. Endoplasmic reticulum stress and the hallmarks of cancer. Trends Cancer. 2016;2:252–62.
14. Senft D, Ronai AZe. Adaptive stress responses during tumor metastasis and dormancy. Trends Cancer. 2016;2:429–42.
15. Kim MP, Lozano G. Mutant p53 partners in crime. Cell Death Differ. 2018;25:161–8.
16. Sabapathy K, Lane DP. Therapeutic targeting ofp53: All mutants are equal, but some mutants are more equal than others. Nat Rev Clin Oncol. 2018;15:13–30.
17. Mantovani F, Collavin L, Del Sal G. Mutant p53 as a guardian of the cancer cell. Cell Death Differ. 2019;26:199–212.
18. Cooks T, Pateras IS, Tarcic O, Solomon H, Schetter AJ, Wilder S, et al. Mutant p53 prolongs NF-κB activation and promotes chronic inflammation and inflammation-associated colorectal cancer. Cancer Cell. 2013;23:634–46.
19. Di Minin G, Bellazzo A, Dal Ferro M, Chiaruttini G, Nuzzo S, Bicciato S, et al. Mutant p53 reprograms TNF signaling in cancer cells through interaction with the tumor suppressor DAB2IP. Mol Cell. 2014;56:617–29.
20. Ingallina E, Sorrentino G, Bertolio R, Lisek K, Zannini A, Azzolin L, et al. Mechanical cues control mutant p53 stability through a mevalonate-RhoA axis. Nat Cell Biol. 2018;20:28–35.
21. Walerych D, Lisek K, Sommaggio R, Piazza S, Ciani Y, Dalla E, et al. Proteasome machinery is instrumental in a common gain-of-function program of the p53 missense mutants in cancer. Nat Cell Biol. 2016;18:897–909.
22. Vogiatzi F, Brandt DT, Schneikert J, Fuchs J, Grikscheit K, Wanzel M, et al. Mutant p53 promotes tumor progression and metastasis by the endoplasmic reticulum UDPase ENTPD5. Proc Natl Acad Sci USA. 2016;113:E8433–42.
23. Wang Y, Shen J, Arenzana N, Tirasophon W, Kaufman RJ, Prywes R. Activation of ATF6 and an ATF6 DNA binding site by the endoplasmic reticulum stress response. J Biol Chem. 2000;275:27013–20.
24. Montibeller L, de Belleroche J. Amyotrophic lateral sclerosis (ALS) and Alzheimer's disease (AD) are characterised by differential activation of ER stress pathways: focus on UPR target genes. Cell Stress Chaperones. 2018;23:897–912.
25. Silwal-Pandit L, Vollan HKM, Chin SF, Rueda OM, McKinney S, Osako T, et al. TP53 mutation spectrum in breast cancer is subtype specific and has distinct prognostic relevance. Clin Cancer Res. 2014;20:3569–80.
26. Liu J, Lichtenberg T, Hoadley KA, Poisson LM, Lazar AJ, Cherniack AD, et al. An integrated TCGA pan-cancer clinical data resource to drive high-quality survival outcome analytics. Cell. 2018;173:400–16 e11.
27. Adachi Y, Yamamoto K, Okada T, Yoshida H, Harada A, Mori K. ATF6 is a transcription factor specializing in the regulation of quality control proteins in the endoplasmic reticulum. Cell Struct Funct. 2008;33:75–89.
28. Li D, Marchenko ND, Moll UM. SAHA shows preferential cytotoxicity in mutant p53 cancer cells by destabilizing mutant p53 through inhibition of the HDAC6-Hsp90 chaperone axis. Cell Death Differ. 2011;18:1904–13.
29. Guan M, Fousek K, Jiang C, Guo S, Synold T, Xi B, et al. Nelfinavir induces liposarcoma apoptosis through inhibition of regulated intramembrane proteolysis of SREBP-1 and ATF6. Clin Cancer Res. 2011;17:1796–806.
30. Guan M, Su L, Yuan Y-C, Li H, Chow WA. Nelfinavir and nelfinavir analogs block site-2 protease cleavage to inhibit castration-resistant prostate cancer. Sci Rep. 2015;5:9698.
31. Gallagher CM, Walter P. Ceapins inhibit ATF6α signaling by selectively preventing transport of ATF6α to the Golgi apparatus during ER stress. eLife. 2016;5:1–24.
32. Chou TC. Theoretical basis, experimental design, and computerized simulation of synergism and antagonism in drug combination studies. Pharm Rev. 2006;58:621–81.
33. Ogata M, Hino S-i, Saito A, Morikawa K, Kondo S, Kanemoto S, et al. Autophagy is activated for cell survival after endoplasmic reticulum stress. Mol Cell Biol. 2006;26:9220–31.
34. Tay KH, Luan Q, Croft A, Jiang CC, Jin L, Zhang XD, et al. Sustained IRE1 and ATF6 signaling is important for survival of melanoma cells undergoing ER stress. Cell Signal. 2014;26:287–94.
35. Zeng L, Lu M, Mori K, Luo S, Lee AS, Zhu Y, et al. ATF6 modulates SREBP2-mediated lipogenesis. EMBO J. 2004;23:950–8.
36. Yao X, Liu H, Zhang X, Zhang L, Li X, Wang C, et al. Cell surface GRP78 accelerated breast cancer cell proliferation and migration by activating STAT3. PLoS ONE. 2015;10:e0125634.
37. Schewe DM, Aguirre-Ghiso JA. ATF6alpha-Rheb-mTOR signaling promotes survival of dormant tumor cells in vivo. Proc Natl Acad Sci USA. 2008;105:10519–24.
38. Li C, Fan Q, Quan H, Nie M, Luo Y, Wang L. The three branches of the unfolded protein response exhibit differential significance in breast cancer growth and stemness. Exp Cell Res. 2018;367:170–85.
39. Bourougaa K, Naski N, Boularan C, Mlynarczyk C, Candeias MM, Marullo S, et al. Endoplasmic reticulum stress induces G2 cell-cycle arrest via mRNA translation of the p53 isoform p53/47. Mol Cell. 2010;38:78–88.
40. Namba T, Chu K, Kodama R, Byun S, Yoon KW, Hiraki M, et al. Loss of p53 enhances the function of the endoplasmic reticulum through activation of the IRE1alpha/XBP1 pathway. Oncotarget. 2015;6:19990–20001.
41. Cunha DA, Igoillo-Esteve M, Gurzov EN, Germano CM, Naamane N, Marhfour I, et al. Death protein 5 and p53-upregulated modulator of apoptosis mediate the endoplasmic reticulum stress-mitochondrial dialog triggering lipotoxic rodent and human beta-cell apoptosis. Diabetes. 2012;61:2763–75.
42. Puthalakath H, O'Reilly LA, Gunn P, Lee L, Kelly PN, Huntington ND, et al. ER stress triggers apoptosis by activating BH3-only protein Bim. Cell. 2007;129:1337–49.